Mechanical Properties of HSLA Steel Buried Gas Tungsten Arc Weldments

Thick-section A710 steel was successfully welded without edge preparation or the use of filler metal

BY W. E. LUKENS

ABSTRACT. The possibility of welding ASTM A710 Grade A Class 3 high-strength low-alloy steel (HSLA-80) up to 19 mm (0.75 in.) thick by the buried gas tungsten arc process has been investigated. This process eliminates edge preparation, reduces the number of passes required, eliminates the need for filler metal wire, and reduces the total heat input per unit length of finished weldment, when compared to standard industry processes, such as submerged arc welding.

Two gas tungsten arc weldments were fabricated with ASTM A710 high-strength low-alloy steel as autogenous square-groove welds. Forced convective cooling by gas impingement on the weld bead surface was used on one of the weldments to enhance the cooling rate of this high heat input process. The mechanical properties and microstructure of these weldments were evaluated.

The results of microstructure observations and mechanical testing indicate that ASTM A710 can be successfully welded by the autogenous buried gas tungsten arc process. The mechanical properties of the A710 autogenous welds fabricated with and without convective cooling of the weld bead surface were similar to base plate properties, except for slightly lower weld metal yield strength. The weld Charpy V-notch energy values ranged widely, but the higher values were close to those of the base plate, except at −51°C (−60°F), where they were lower. The ASTM A710 weldment produced with convective cooling to enhance the cooling rate had higher Charpy V-notch energy values than the weldment produced without convective cooling.

W. E. LUKENS is with the David Taylor Research and Development Center, Bethesda, Md.

Paper presented at the 67th Annual AWS Meeting, held April 13-18, 1986, in Atlanta, Ga.

Introduction

The welding processes extensively used for joining thick-walled components such as forgings, pressed or spun-end closures, shapes, castings, and plate necessitate edge preparation with a large included angle (45 to 60 deg) (Ref. 1). Research and development work aimed at eliminating edge preparation is currently under way in the area of narrow groove joints (Ref. 2). Another method to eliminate edge preparation is to weld with a nonconsumable electrode and with the arc immersed. This method is known as the buried gas tungsten arc welding process.

The use of this process was first reported (Ref. 3) by the Soviets in 1964, where results were given concerning research into the buried GTAW of titanium alloys. Butt joint weldments in 25.4-mm (1-in.) thick plate were fabricated in only four passes without any edge preparation. In the following year, an investigator from the United States reported (Ref. 4) the use of this process for welding aluminum. Butt joint weldments in 31.8-mm (1¼-in.) thick plate were fabricated in only two autogenous passes without any edge preparation. Liptak reported (Ref. 4) that the greatest single cost advantage arose from the elimination of filler metal.

There are few references to the application of this process to steel welding. Shtrikman (Ref. 5) investigated the possibility of welding Types VNS2 and 30KhGSA steels up to 22.1 mm (0.87 in.) in thickness by the buried GTAW process. The 30KhGSA is a medium-alloy steel, and the VNS2 is a heat-resistant stainless steel containing age-hardenable martensite (Ref. 6). Acceptable weld fusion zone and heat-affected zone (HAZ) properties were obtained in the 30KhGSA steel and the VNS2 steel after a postweld heat treatment. In 1982, another Soviet article (Ref. 7) stated that this process was used extensively in Soviet industry in the welding of various metals because the welding equipment is simple, it is possible to weld large components, and requirements on the variation of the welding root opening are not stringent.

Because of the high potential for production welding cost reduction by the buried GTAW process through elimination of edge preparation, reduction in the number of passes required, elimination of the need for filler metal, and reduction in the total heat input per unit length of finished weldment, this process could be competitive with submerged arc welding (SAW) for application to high-strength steels. This paper presents an analysis of the benefits and feasibility of the process, the development of welding variables, and the mechanical properties of buried GTAW weldments in ASTM A710 Grade A Class 3 high-strength low-alloy (HSLA-80) steel.

KEY WORDS

Buried GTA Weldments
Forced Convection
Convective Cooling
Gas Impingement
Immersed GTAW Arc
Buried Autog GTAW
ASTM 710 HSLA Steel
Low Arc Voltage GTAW
Autogenous GTA Welds
NDT Inspectn Results

Materials and Procedures

The material selected for this investigation was ASTM A710 Grade A Class 3 high-strength low-alloy steel with the following analysis in wt-%: carbon – 0.05, manganese – 0.51, phosphorus – 0.004, sulfur – 0.008, silicon – 0.34, nickel – 0.95, chromium – 0.66, molybdenum – 0.21, copper – 1.25, columbium – 0.040, aluminum – 0.037, and nitrogen – 0.009, with iron as the balance.

All plates were 19 mm (0.75 in.) thick

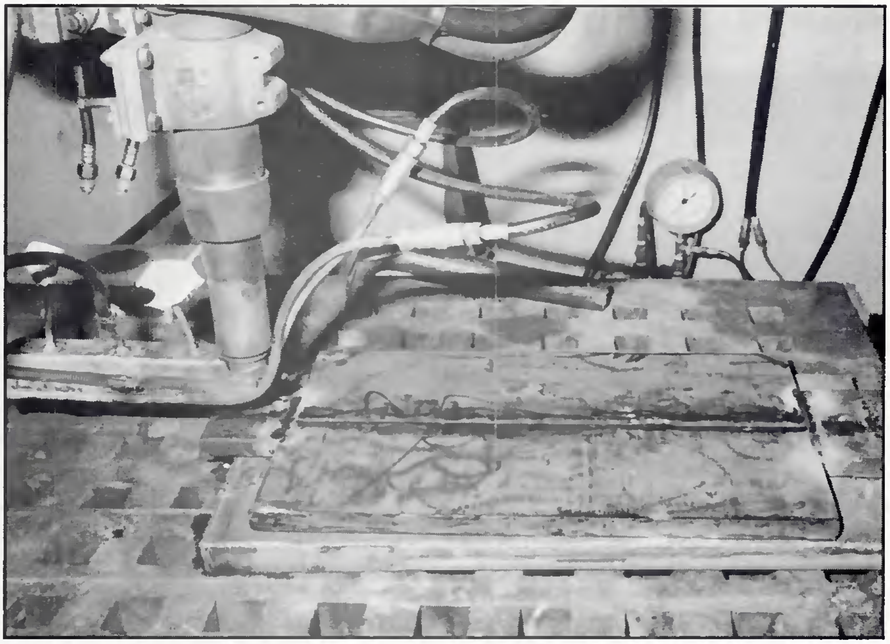

Fig. 1—Plate assembly prior to buried gas tungsten arc welding

and were cut into 438- × 152-mm (19- × 6-in.) pieces with the short edge lying in the longitudinal (L) or rolling direction. The longitudinal surface of the edge of the plates to be welded was ground to remove the flame cut surface. Two plates were tack welded to form a square-groove in a butt joint with no root opening. The plate assembly before welding is shown in Fig. 1.

The buried GTAW process employs a high welding current with a low arc voltage to displace the molten weld pool beneath the tungsten electrode, thus permitting the tungsten to penetrate beneath the plate surface until the arc pressure is offset by the weight of the displaced molten metal. Two buried GTA weldments were fabricated in ASTM A710 steel as autogenous square-groove welds. The welds were made with a 6.4-mm (0.25-in.) thoriated tungsten electrode. To enhance penetration, helium was added to the argon torch gas to produce a mixture of 80% helium and 20% argon. Arc current was maintained at 1000 A, arc voltage at 12 V, and torch travel speed at 2.0 mm/s (4.75 ipm). The square-groove weldments in 19-mm (0.75-in.) thick plate were made in the flat position in two passes, one from each side. Forced convective cooling by gas impingement on the weld bead surface as developed by Wells (Ref. 8) was used on one ASTM A710 weldment to enhance the cooling rate of this high heat input process. The convective cooling device is shown attached to the welding torch in Fig. 1. The welding variables for each weld pass are shown in Table 1.

Table 1—Variables Employed for Buried Gas Tungsten Arc Welding of Steel

Weldment identification	BA6		BA7	
Base plate material	ASTM A710 Grade A, Class 3		ASTM A710 Grade A, Class 3	
Welding position	flat		flat	
Joint design	square groove		square groove	
Filler metal wire	none—autogenous		none—autogenous	
Welding polarity	DCEN		DCEN	
Machine characteristics	CC		CC	
Tungsten electrode diameter (mm)	6.4 2% thoriated		6.4 2% thoriated	
Torch shield gas	13.7 Ar 63.7 He		13.7 Ar 63.7 He	
Convective cooling gas	18.2 He		273 He	
Preheat (°C)	22		22	
Welding pass	1	2	1	2
Welding current (A)	1000	1030	1000	1000
Arc voltage (V)	12.5	12	12	12
Torch travel speed (mm/s)	2.0	2.0	2.0	2.0
Heat input (kJ/mm)	6.2	6.1	6.0	6.0

Weldment Characterization Procedures

Following welding, the weldments were magnetic particle inspected to determine surface defects, such as cracking, and radiographed to determine internal defects, such as porosity and/or cracking.

The buried GTA weldments were optically examined for microstructure. The microstructure examination included the base plate material, the HAZ, and the fusion zone. Chemical analysis was performed on the fusion zone. Microhardness tests were made on transverse cross-sections of the weld 6.4 mm (¼ in.) from the surface of the second side, and also from surface to surface through thickness along the weld centerline.

The mechanical properties of these weldments were evaluated. The mechanical properties included yield strength, ultimate tensile strength, elongation, reduction of area, and fracture toughness. The fracture toughness of the welds was determined by the Charpy V-notch (CVN) impact test. The CVN tests were conducted at −51°C (−60°F) and −18°C (0°F).

Results

Magnetic particle inspection of the finished weldments showed no evidence of surface cracking. Similarly, radiographic inspection showed no indications of cracking, porosity, or tungsten inclusions.

All square-groove weldments were made in two passes, one from each side. Penetration of approximately 13 mm (0.5 in.) per pass was achieved, which resulted in a 7 mm (0.28 in.) overlap at the weld root. The completed weldment, BA6, is shown in Fig. 2, and macrosections from both weldments are shown in Fig. 3.

The microstructure of the A710 base plate shows the presence of polygonal ferrite with dark areas, which are probably pearlite—Fig. 4A. The HAZ near the base plate consists of fine-grained polygonal ferrite plus the dark-etching microconstituent, which is probably pearlite—Fig. 4B. The HAZ near the fusion zone consists of a light-etching matrix phase, which is probably bainitic ferrite—Fig. 4C. Dispersed throughout the bainitic ferrite are higher carbon regions, which appear dark. These regions consist of cementite particles and martensite-austenite (MA). The fusion zone of both buried GTA weldments are shown in Fig. 5. The enhanced cooling by forced convection (Weldment BA7) did not affect the optical microstructure. Both weldments have fusion zones which consist of ferrite veins, acicular ferrite, and bainite.

The results of interstitial chemical anal-

Table 2—Interstitial Fusion Zone Composition, A710 Weldments (wt-%)

Weldment Indentification	C	O	N	H
BA6	0.036	0.011	0.011	0.00003
BA7	0.036	0.009	0.009	0.00004
Base plate	0.05	—	0.009	—

ysis of the fusion zone material is shown in Table 2. The difference between BA6 (no convective cooling) and BA7 (convective cooling) with regard to oxygen and nitrogen is very slight. Carbon and hydrogen are essentially the same.

Microhardness surveys from the fusion zone to the base plate for Weldments BA6 and BA7 are shown in Fig. 6. Convective cooling does not appear to affect hardness. The average fusion zone hardness for BA6 is 228 and for BA7 is 226. It can be seen that there is a distinct softening in the HAZ, which is consistent with findings on lower heat input GTA autogenous weldments produced in this material (Ref. 9). Microhardness surveys from one plate surface to the other surface through the plate thickness along the weld centerline were also taken, as shown in Fig. 7. The fused metal from the first pass (which was heat affected by the second pass) did not exhibit the softening that was observed in the base plate HAZ.

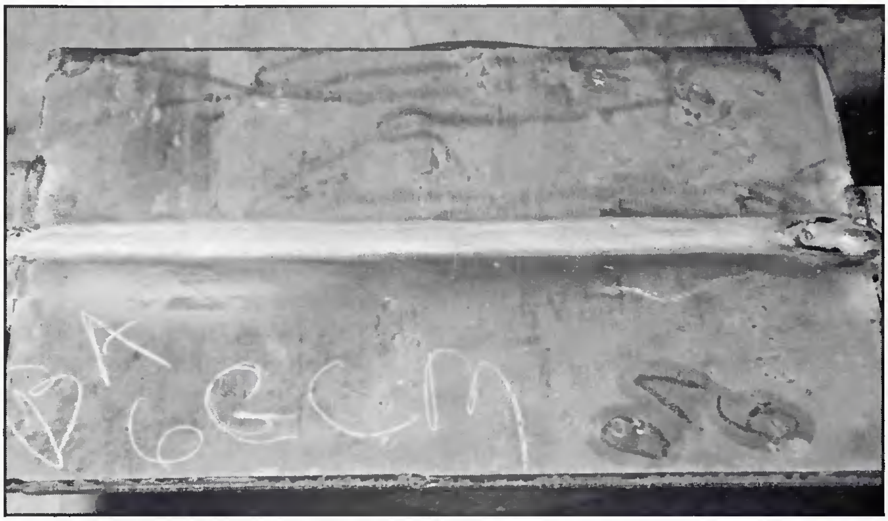

Fig. 2—Completed buried gas tungsten arc weldment in ASTM A710 steel (Weldment BA6)

The mechanical properties of the ASTM A710 welds are shown in Table 3. Typical plate properties and autogenous laser beam welding (LBW) fusion zone properties from a previous study (Ref. 10) are shown for comparison. The yield strengths for LBW and both GTA weld-

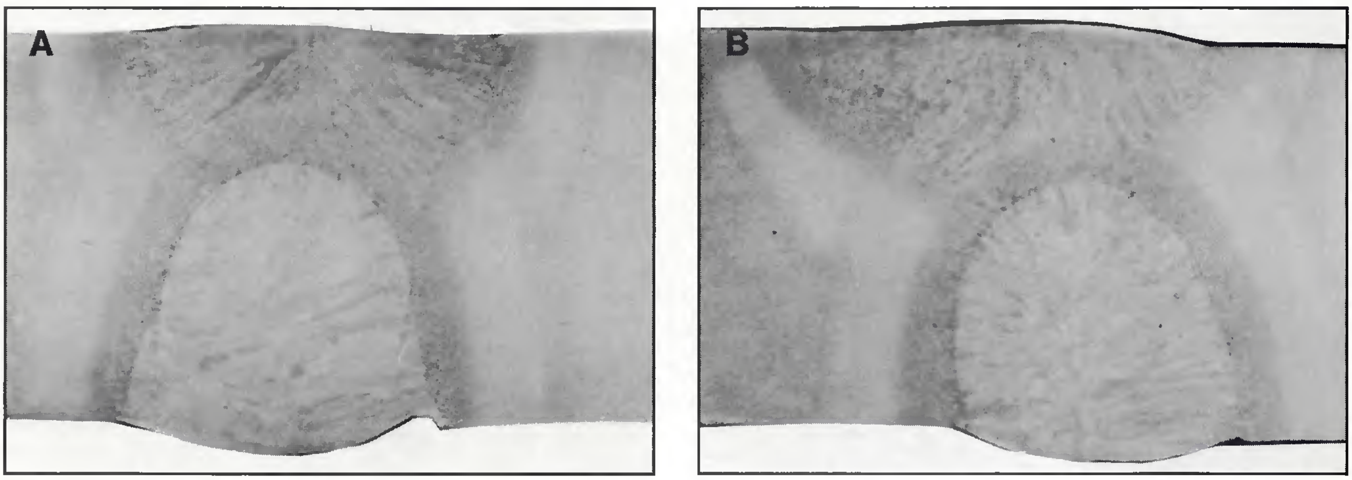

Fig. 3—Photomacrographs showing buried GTA autogenous weld shapes. A—BA6 ASTM A710; B—BA7 ASTM A710 (convective cooling)

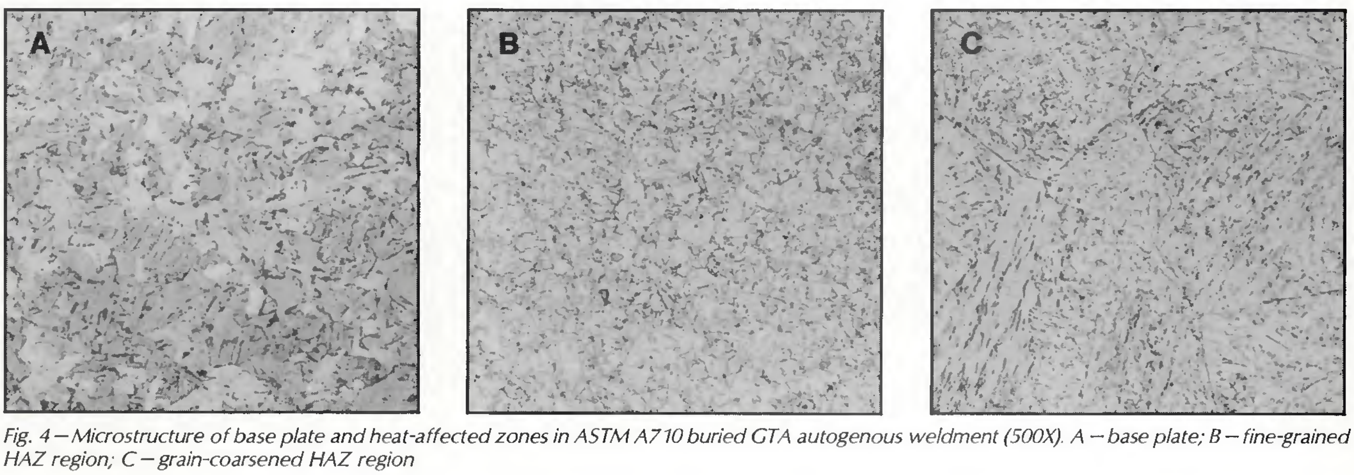

Fig. 4—Microstructure of base plate and heat-affected zones in ASTM A710 buried GTA autogenous weldment (500X). A—base plate; B—fine-grained HAZ region; C—grain-coarsened HAZ region

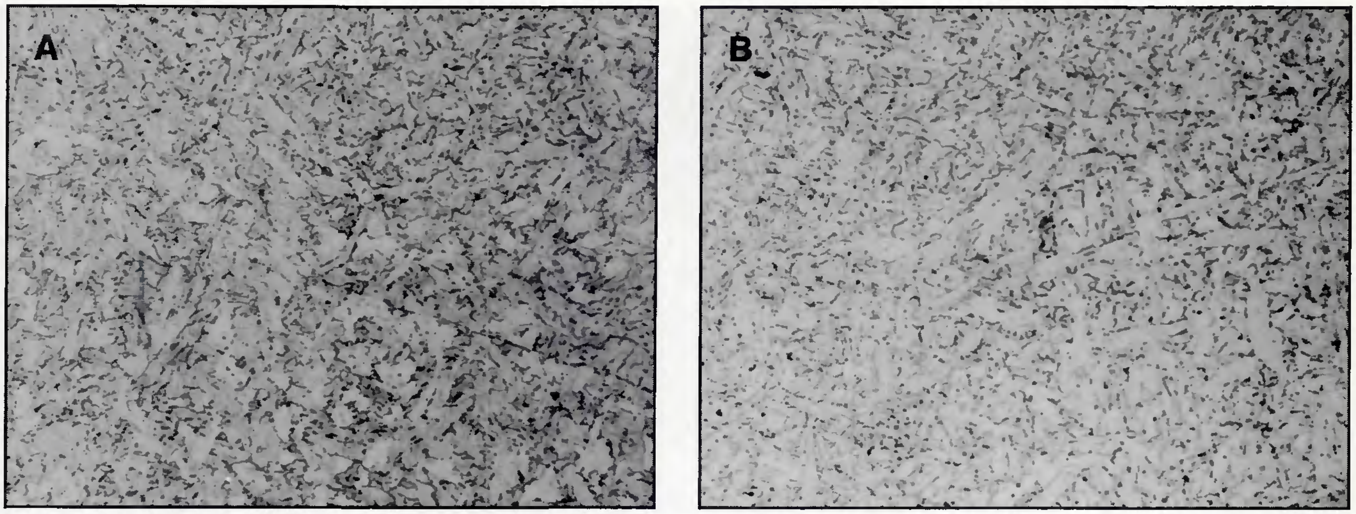

Fig. 5—Microstructure of fusion zone in ASTM A710 buried GTA autogenous weldments (500X). A—Weldment BA6, no convective cooling; B—Weldment BA7, convectively cooled

ments were similar, and somewhat lower than base plate properties. The ultimate tensile strengths of Weldments BA6 and BA7 base plate were similar, while that of the laser beam weldment was lower. Ductility of the BA6 and BA7 weldments was similar to base plate ductility, while that of the laser beam weldment was lower.

The CVN results for buried GTAW, LBW (Ref. 10), and the base plate all showed scatter over a large range. These results are presented in Fig. 8. In order to draw the plate curve, the data for each temperature were averaged and a curve smoothing routine was employed. Some of the scatter in the GTA welds is a consequence of specimen location, the higher values being obtained from specimens which were removed from the as-deposited second weld pass, while the lower values were obtained from specimens which included material from the reheated first pass. No attempt was made in this work to separately characterize the properties of each weld pass. The BA7 weldment, produced with convective cooling to enhance the cooling rate, had higher CVN energy values than the weldment produced without convective cooling.

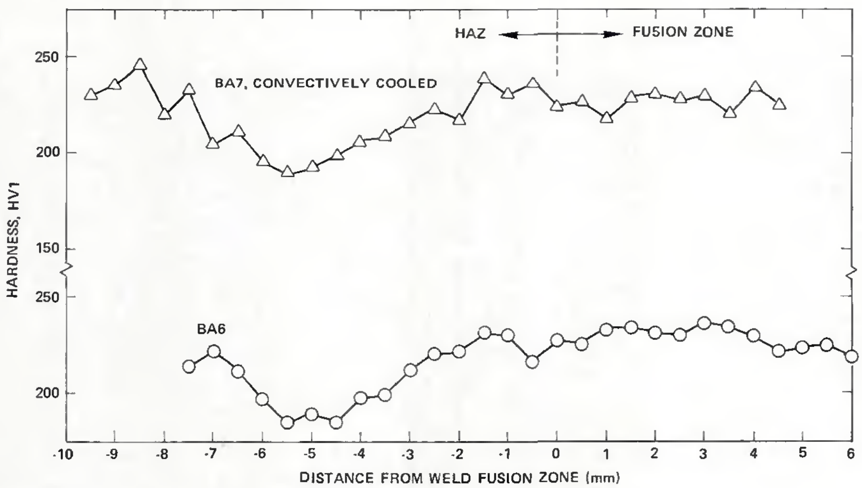

Fig. 6—Microhardness profiles of A710 buried GTA autogenous welds

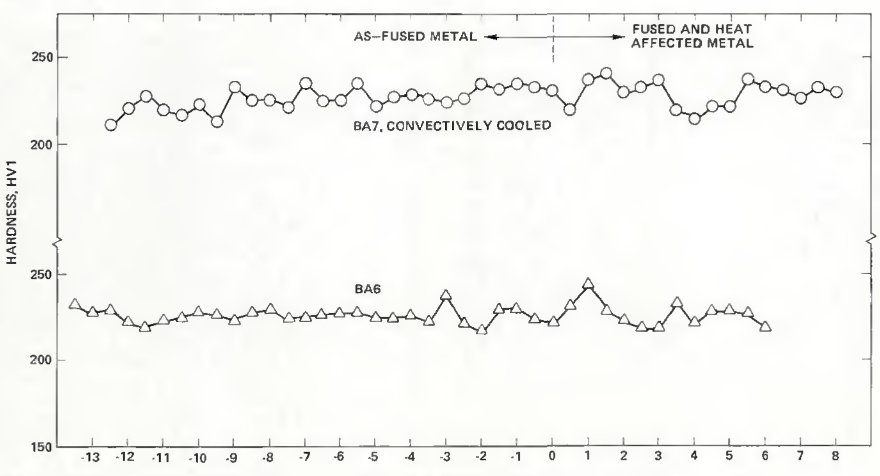

Fig. 7—Fusion zone microhardness profiles of A710 buried GTA autogenous welds

Discussion

The results show that sound autogenous welds, free from defects, can be produced in ASTM A710 HSLA steel.

The hardness minimum in the baseplate HAZ is located in the outer part of the intercritical region. Overaging and re-solution of the copper precipitates, and the redistribution of carbon into coarse MA and bainite islands, caused the reduced hardness (Ref. 9).

The fusion zone mechanical properties of the autogenous buried GTA weldments in ASTM A710 steel are not adversely affected, and compare favorably with base plate properties. The large range of CVN values for the A710 welds indicated a possible weld discontinuity-related problem. However, visual observations of the fracture surfaces failed to support this hypothesis. The fracture surfaces were clean, with no indications of cracking, porosity, tungsten inclusions, or incomplete fusion which may have